HEFAT2008
6th International Conference on Heat Transfer, Fluid Mechanics and Thermodynamics
30 June to 2 July 2008
Pretoria, South Africa
Paper number: K2

THEORETICAL AND EXPERIMENTAL STUDIES IN SHELL-SIDE CONDENSATION

Briggs A.
School of Engineering and Materials Science
Queen Mary, University of London
London, E1 4NS
United Kingdom
E-mail: a.briggs@qmul.ac.uk

ABSTRACT

The fundamental phenomena behind condensation on simple banks of plain tubes and free and forced convection condensation on single integral-fin tubes are examined. This is followed by a detailed evaluation of available theoretical models and empirical correlations.

Throughout the paper, a strong emphasis is placed on quantitative evaluation of predictive methods. For example, in the case of condensation on banks of plain tubes a data base of nearly five thousand points, covering 6 test fluids and 13 tube bank geometries is compared to theoretical models available in the literature.

Finally, gaps in the available knowledge are highlighted and it is hoped that this will help stimulate further work on these areas.

INTRODUCTION

The condenser is a major component of process, refrigeration and power plant. Major reductions in capital cost can be achieved by improvements to design leading to smaller units. Increased condenser performance can also lead to significant increases in cycle efficiency of power plants by reducing turbine exhaust pressure.

A program of condenser research has been in progress at Queen Mary, University of London for some time and the author has been involved in many aspects of this work for nearly twenty years. The work includes experimental and theoretical work on both shell-side and tube-side condensation. This paper will concentrate on two areas of this work; namely condensation on banks of plain tubes and condensation on integral-fin tubes.

NOMENCLATURE

A	Empirical constant in equations (35) and (36)
A_1, A_2	Parameters in equation (13)
a	Empirical constant in equations (35) and (36)
a_1, a_2	Empirical constants in equation (13)
B, B_1	Empirical constants in equation (25)
b	Fin spacing at fin tip
C	Parameter in equation (31)
C_1, C_2	Constants in equation (9)
c_P	Specific heat capacity
d	Diameter of smooth tube or fin-root diameter of finned tube
d_o	Diameter at fin tip
F	Dimensionless parameter, $(\mu g d h_{fg}/k U_{mv}^2 \Delta T)$
f_f	fraction of fin flank "blanked" by condensate "wedge"
f_s	fraction of interfin tube surface "blanked" by condensate "wedge"
G	Mass velocity, $U_v \rho_v$
g	Specific force of gravity
h	Radial fin height
h_{fg}	Specific enthalpy of evaporation
h_v	Mean vertical fin height (see equations (26) and (27))
J_v	Dimensionless parameter (see equation (5))
j	Constant in equation (6)
k	Thermal conductivity
k_w	Thermal conductivity of tube
M	Empirical constant in equation (36)
m	Empirical constant in equation (13)
N	Empirical constant in equation (30)
N_{tot}	Number of data points
Nu	Nusselt number, $\alpha d/k$
Nu_l	Nusselt number based on liquid flowing alone in bank
n	Empirical constant in equation (13), (14) and (15)
P	Pressure
P_t, P_l	Transverse and longitudinal tube pitchs
Pr	Prandtl number, $\mu c_P/k$
p	Fin pitch
q	Heat flux based on area of plain tube with fin root diameter
Re_{eq}	"Equivalent" Reynolds number, defined by equation (32)
Re_{fgr}	Film Reynolds number based on gravity drained flow
Re_{fu}	Film Reynolds number based on uniformly distributed flow
$Re_{l,max}$	Reynolds number for liquid flowing alone through bundle and based on maximum velocity (i.e. through minimum cross-sectional area between the tubes)
$Re_{v,max}$	Vapour Reynolds number based on maximum velocity $\rho_v U_{max} d/\mu_v$
$Re_{tp,max}$	Two-phase Reynolds number based on maximum velocity, $\rho U_{max} d/\mu$
$Re_{tp,min}$	Two-phase Reynolds number based on minimum velocity, $\rho U_v d/\mu$
$Re_{tp,mv}$	Two-phase Reynolds number based on "means void" velocity, $\rho U_{mv} d/\mu$
r	Local radius of curvature of condensate surface
s	Fin spacing at fin root
t	Fin thickness at fin tip
U_{max}	Vapour velocity based on vapour volume flow rate and minimum cross sectional area of test section (i.e. between adjacent tubes in a row or between single tube and test section wall)
U_{mv}	Vapour velocity based on vapour volume flow rate and "mean-void" cross sectional area of test section (i.e. the total volume of the test

section not occupied by tubes divided by its length in the direction of the flow)

U_v Vapour velocity based on vapour volume flow rate and total cross sectional area of test section (i.e. just upstream of test bank or test tube)

X_{tt} Lockhart-Martinelli parameter

X Coordinate measured along condensate-vapour interface

x Vapour quality

Special Characters

α Vapour-side, heat-transfer coefficient, $q/\Delta T$

β fin tip half angle

Γ Mass flow rate of condensate draining from tube

γ Mass flow rate of fluid condensing on tube

ΔT Vapour-side temperature difference

ε Enhancement ratio (heat-transfer coefficient for finned tube divided by heat-transfer coefficient for smooth tube, both based on smooth tube area at fin root diameter and for same vapour-side temperature difference and vapour velocity)

μ Viscosity

ν Kinematic viscosity

$\xi(\phi_f)$ Function approximated by equation (28)

ρ Density

$\tilde{\rho}$ $\rho - \rho_v$

σ Surface tension

ϕ_f Retention angle measured from top of tube

Subscripts

None Condensate

calc Calculated value

exp Experimental value

gr Pertaining to gravity controlled flow

Nu Calculated from Nusselt [17] theory

root Pertaining to fin root

sh Pertaining to for shear controlled flow

tip Pertaining to fin tip

v Vapour

w Evaluated at outside wall temperature

CONDENSATION ON BANKS OF PLAIN TUBES

For condensation on banks of tubes, the flow pattern is generally three-dimensional and involves complex interactions between vapour and condensate. Heat transfer is effected by condensate inundation and the reduction in vapour velocity down the bank accompanying condensation. A vast amount of experimental data is available in the open literature and the relevant variables have been studied systematically. Furthermore, attempt have been made to incorporate the complex interactions outlined above into theoretical correlations.

Experimental Data Base

Table 1 summarises an extensive experimental data base extracted from the open literature. It includes data for 6 condensing fluids and 13 tube bank configurations extracted from 15 sources. Figure 1 shows schematics of the test section geometries used in the studies. The test sections can be divided into two types; those where the whole test bank is active (with the exception of dummy half tubes on the walls of the triangular test banks) and those where a single active tube is positioned in a bank of dummy tubes. In both cases artificial condensate inundation was sometimes employed to simulate conditions near the bottom of a larger tube bank.

The Model of Shekriladze and Gomelauri [16]

This purely theoretical model was developed for condensation on a single tube in an infinitely wide duct but has shown some success in predicting heat-transfer coefficients for banks of tubes. It provides a useful baseline for comparison with more complex models. The authors used the assumptions of the Nusselt [17] model for free convection on a single tube but added the asymptotic, infinite condensation rate approximation for the shear stress at the condensate-vapour interface. Their result can be represented by the equation of Rose [18] as follows

$$\frac{Nu}{Re_{tp,mv}^{1/2}} = \frac{0.9 + 0.728F^{1/2}}{(1 + 3.44F^{1/2} + F)^{1/4}} \qquad (1)$$

Equation (1) tends to $Nu/Re_{tp,mv}^{1/2} = 0.9$ for small F (high vapor velocity) while at large F (low vapour velocity) it tends to the result of Nusselt [17], which can be written as

$$\frac{Nu}{Re_{tp,mv}^{1/2}} = 0.728F^{1/4} \qquad (2)$$

Before comparing the whole experimental data set to equation (1) it is worthwhile comparing the model to data with a vapour quality of 1 upstream of the test tubes, i.e. data where no condensate, either artificial or generated by other active tubes, is present. This reduced data set consists mainly of data for the top row of the various tube banks but also, in the case of the data of Nobbs [1], Gogonin and Dorokhov [6, 7] and Beech [3], data set 3, where a single active tube was positioned in a dummy bank and the case of Beech [3], data set 1, where rows of dummy tubes were positioned upstream of the first active row (see Figure 1). The comparison is shown in Figure 2, where the vapour velocity used is based on the vapour mass flow rate just upstream of the tubes and the "mean void" area of the test section, i.e. the total volume of the test section not occupied by tubes divided by its length in the direction of the flow. Three sets of data stand out in Figure 2. Those of Kutataladze et al. [11] are above the theoretical line and show a large degree of scatter, while the data of Briggs and Bui [5] and Shah [10] are below the theoretical prediction. The rest of the data are in relatively good agreement with the theoretical line of Sheriladze and Gomelauri [16] for low vapour velocities (high values of F) but show a distinctive upturn in the values of $Nu/Re_{tp}^{0.5}$ at values of F below 1 and 0.1 for steam and non-steam data respectively. This may suggest transition to turbulent flow in the condensate film.

When all the available data are compared to equation (1) the situation not surprisingly becomes more complex. Figures 3a and b show the steam and non-steam data respectively. In both cases much of the data (with the marked exception of those of Kutataladze et al. [11]) are below the Shekriladze and Gomelauri [16] line suggesting that condensate inundation is having a measurable and negative effect on the heat transfer. For the steam data the upturn in the data at low values of F is even more marked. Condensate inundation from tube rows higher up the bank onto those below produces higher film

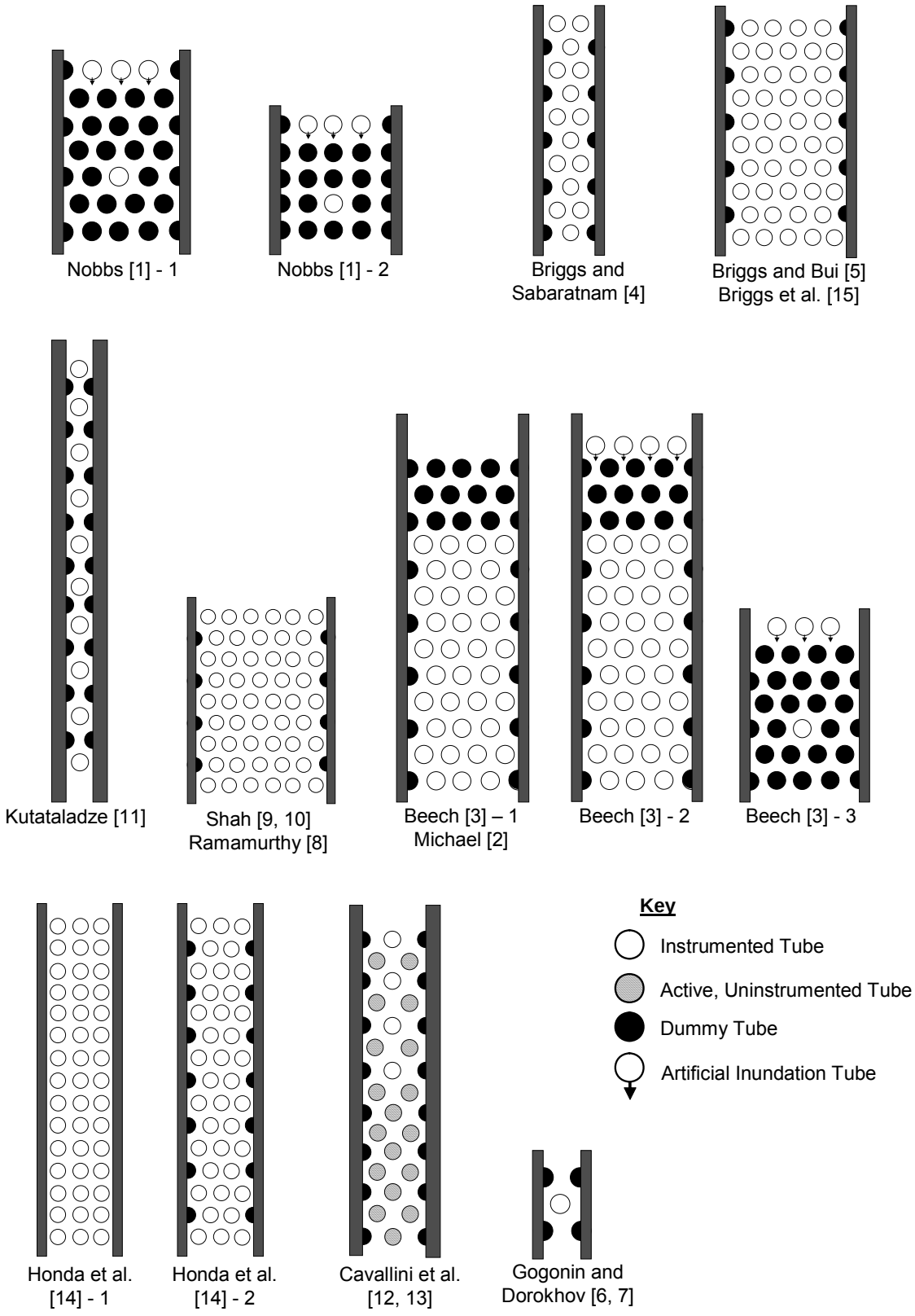

Figure 1 Schematics of Test Banks

Table 1 Condensation on Banks of Plain Tubes - Experimental Data Base

Reference	Fluid	Bank layout	Tube outside diameter / mm	Vapour velocity* / (m/s)	Symbols used in Figures
Nobbs [1] - 1	Steam	Triangular (SAT, ACI)	19.1	0.3 - 9.2	♦
Nobbs [1] - 2	Steam	Square (SAT, AI)	19.1	0.4 - 8.3	◊
Michael et al. [2]	Steam	Triangular	14.0	6.0 - 21.6	*
Beech [3] - 1	Steam	Triangular	14.0	6.1 - 18.3	▲
Beech [3] - 2	Steam	Triangular (ACI)	14.0	6.1 - 19.6	-
Beech [3] - 3	Steam	Triangular (SAT, ACI)	14.0	4.2 - 10.2	△
Briggs and Sabaratnam [4]	Steam	Triangular	19.1	4.5 - 10.6	□
Briggs and Bui [5]	Steam	Triangular	18.7	1.5 - 4.1	x
Gogonin and Dorokhov [6]	R-21	Triangular (SAT)	17.0	0.1 - 0.2	△
Gogonin and Dorokhov [7]	R-21	Triangular (SAT)	17.0	0.1 - 2.0	▲
Ramamurthy [8]	Iso-propanol	Triangular	12.7	0.4	-
Shah [9]	Iso-propanol	Triangular	12.7	0.4 - 0.5	*
Shah [10]	Methanol	Triangular	12.7	0.4 - 0.6	x
Kutataladze et al. [11]	R-21	Triangular (SAT)	16.0	0.2 - 1.7	+
Cavallini et al. [12]	R-11	Triangular	10.0	0.5 - 4.3	□
Cavallini et al. [13]	R-113	Triangular	10.0	0.9 - 5.1	■
Honda et al. [14] - 1	R-113	Square	15.9	0.6 - 5.4	o
Honda et al. [14] - 2	R-113	Triangular	15.9	0.6 - 5.6	●
Briggs et al. [15]	R-113	Triangular	18.7	0.1 - 0.4	◊

* At Approach to Test Bank
SAT - Single Active Tube
ACI - Artificial Inundation

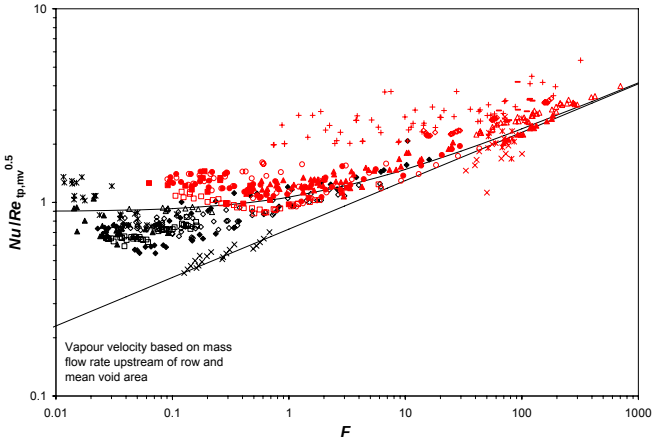

Figure 2 Comparison of Model of Shekriladze and Gomelauri [16] to Experimental Data with No Inundation (For key see Table 1)

Reynolds numbers which may further promote the onset of turbulence in the condensate film.

The Model of Cavallini et al. [19]

Cavallini added a correction to the Shekriladze and Gomelauri [16] model to account for the effect of condensate inundation as follows,

$$\frac{Nu}{Re_{tp,mv}^{1/2}\left(\frac{\Gamma}{\gamma}\right)^{-0.16}} = \frac{0.9+0.728F^{1/2}}{(1+3.44F^{1/2}+F)^{1/4}} \qquad (3)$$

The correction was based on work by Cipollone et a. [20] for condensation of low velocity vapour on staggered tube banks. Figures 4a and b show the data plotted on the basis of equation (3). The correction for condensate inundation shifts the

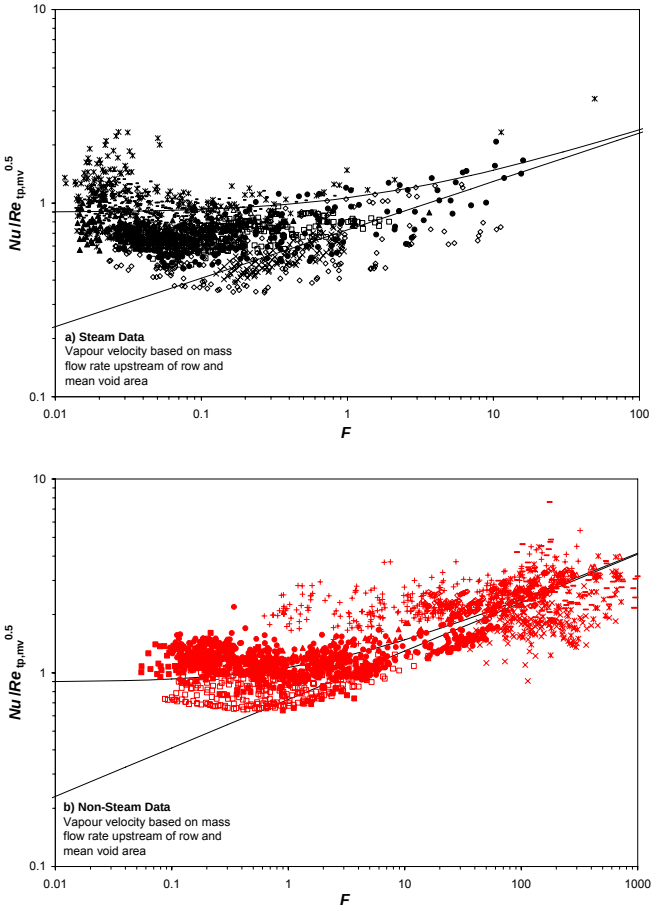

Figure 3 Comparison of Model of Shekriladze And Gomelauri [16] to Experimental Data (For key see Table 1)

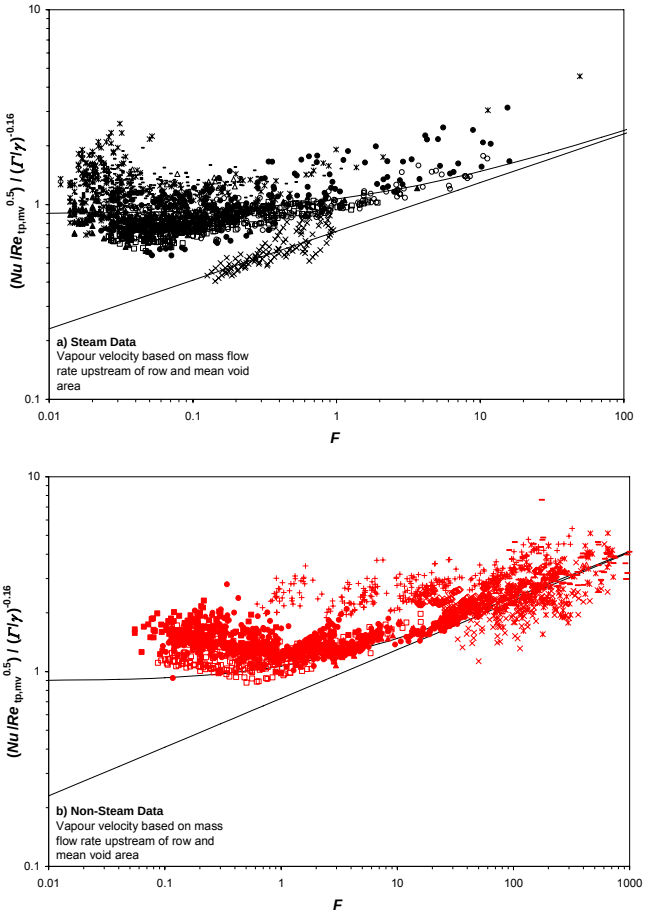

Figure 4 Comparison of Model of Cavallini [19] to Experimental Data (For key see Table 1)

data upwards and moves them, in most cases, above the theoretical line. The data of Nobbs [1] are particularly effected. The exceptions are the data of Briggs and Bui [5] and Shah [10] which are characterised by low inundation rates and therefore are hardly effected by the correction. There is suspicion here that the data may be effected by air in the test section, particularly at low vapour velocities and towards the bottom of the banks

The Model of M^{c}Naught [21]

M^{c}Naught [21] examined the interaction between vapour shear and gravity and suggested the following equation to calculate their combined effect.

$$Nu = \left(Nu_{gr}^2 + Nu_{sh}^2\right)^{1/2} \qquad (4)$$

The form of equation (4), where two extreme values of Nusselt number are combined on a power basis, has no real physical basis but is often used to great effect in heat-transfer correlations. A dimensionless parameter, J_v, was suggested to indicate the relative importance of vapour shear and gravity effects

$$J_v = \frac{x\,G}{\sqrt{dg\rho_v\left(\rho-\rho_v\right)}} \qquad (5)$$

Based on data of Nobbs [1] were $J_v < 1.5$, M^{c}Naught [21] suggested the following approximate expression for the gravity-controlled region.

$$Nu_{gr} = Nu_{Nu}\left(\frac{\Gamma}{\gamma}\right)^{-j} \qquad (6)$$

where $j = 0.22$ for square banks and 0.13 for triangular banks.

For the shear-controlled region an empirical equation based on data of Nobbs [1] were $J_v > 1.5$ was proposed, as follows,

$$Nu_{sh} = 1.26\,Nu_l\left(\frac{1}{X_{tt}}\right)^{0.78} \qquad (7)$$

where X_{tt} is the the Lockhart-Martinelli parameter.

$$X_{tt} = \left(\frac{1-x}{x}\right)^{0.9}\left(\frac{\rho_v}{\rho}\right)^{0.5}\left(\frac{\mu}{\mu_v}\right)^{0.1} \qquad (8)$$

and Nu_l is the Nusselt number calculated as if the liquid was flowing alone through the bundle, from [22] as follows,

$$Nu_l = C_1\left(Re_{l,max}\right)^{C_2} Pr^{0.34}\left(\frac{\mu c_P k_w}{\mu_w c_{Pw} k}\right)^{0.26} \qquad (9)$$

$Re_{l,max}$ is based on the maximum velocity (i.e. through the minimum flow area between the tubes),

$C_1 = 1.309$ and $C_2 = 0.360$ when $Re_{l,max}$ 10 $\leq$ 300
$C_1 = 0.273$ and $C_2 = 0.635$ when $300 < Re_{l,max} \leq 2\text{x}10^5$
$C_1 = 0.124$ and $C_2 = 0.700$ when $Re_{l,max} > 2\text{x}10^5$

Figures 5a and b compare the M^{c}Naught [21] model with the data for steam and other fluids respectively. Agreement is not good. For steam the model over predicts the data of Briggs and Bui [5] by as much as 100%, although this may be due to problems with the experimental data mentioned earlier. The significant under prediction of the data of Beech [3] and Michael [2] is perhaps more serious. It should be noted that the correlation was based on only the data of Nobbs (which it agrees with quite well) while much of the other data is for higher vapour approach velocities. This highlights the danger of extrapolating a correlation beyond the range of physical parameters used in its development. For the non-steam data the correlation over predicts much of the data; the exception being that of Kutataladze et al. [11].

The Model of Honda et al. [14]

Honda et al. [14] studied condensate flow characteristics within tube bundles and introduced gravity drained and uniformly dispersed flow models to estimate the condensate inundation rate at low and high vapour velocities respectively. In the former, which might be expected when vapour shear is low, all condensate is assumed to fall onto the tube directly below (i.e. in the next row for inline bundles and two rows down the bank for staggered bundles) while in the latter (at higher vapour shear) the condensate is assumed to be uniformly distributed across the test section normal to the flow and hence only a fraction of the condensate impinges on the tubes below. Semi-empirical equations for determining the heat-transfer coefficient of tube bundles were obtained by combining correlations for gravity-controlled and shear controlled regimes. For in-line bundles, the heat-transfer coefficient was determined using

$$Nu = \left(Nu_{gr}^4 + Nu_{sh}^4\right)^{1/4} \qquad (10)$$

and for staggered bundles using

$$Nu = \left(Nu_{gr}^4 + Nu_{gr}^2 Nu_{sh}^2 + Nu_{sh}^4\right)^{1/4} \qquad (11)$$

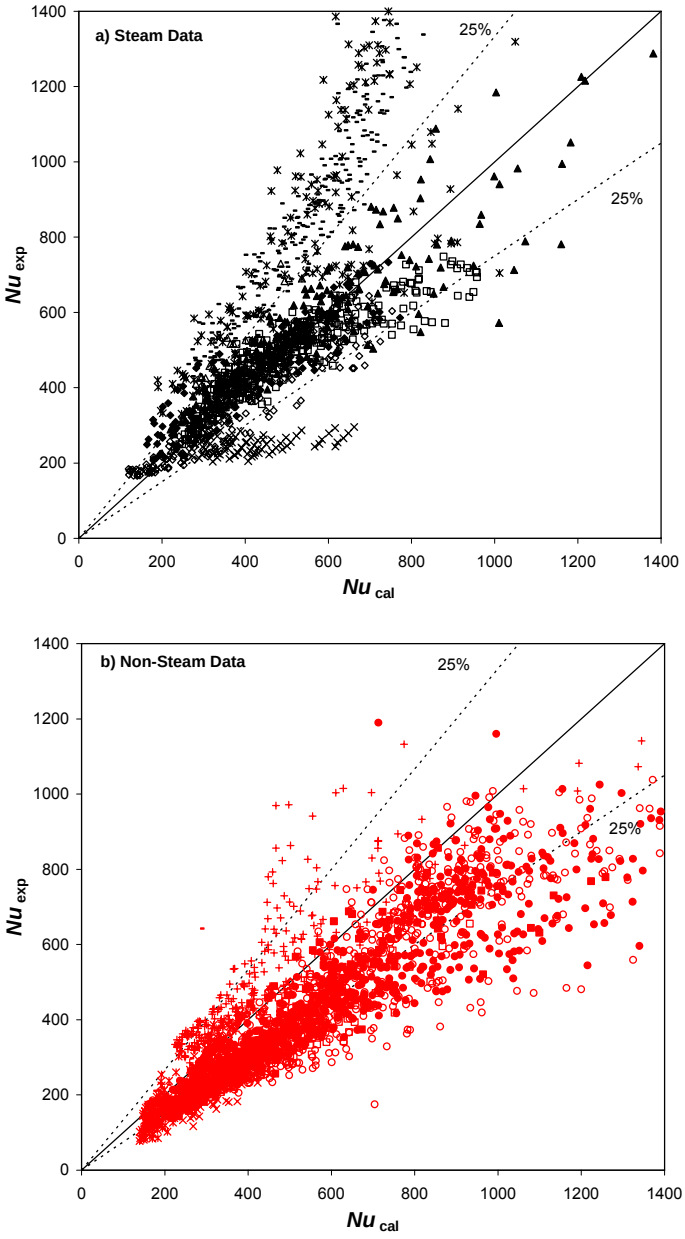

Figure 5 Comparison of Model of M^{c}Naught [21] to Experimental Data (For key see Table 1)

where Nu_{gr} is the Nusselt number for the gravity-controlled regime given by

$$Nu_{gr} = d\left(\frac{g}{\nu^2}\right)^{1/3}\left(2.1Re_{f,gr}^{-1.2} + 2.7\text{x}10^{-5} Re_{f,gr}^{0.8}\right)^{1/4} \qquad (12)$$

$Re_{f,gr}$ is the film Reynolds number calculated under the assumption of gravity-controlled flow. Equation (12) was based on the low vapour velocity data of Kutateladze and Gogonin [23] and Kutateladze et al. [24], for R-12 and for R-21. Nu_{sh} is the Nusselt number for shear controlled flow given by

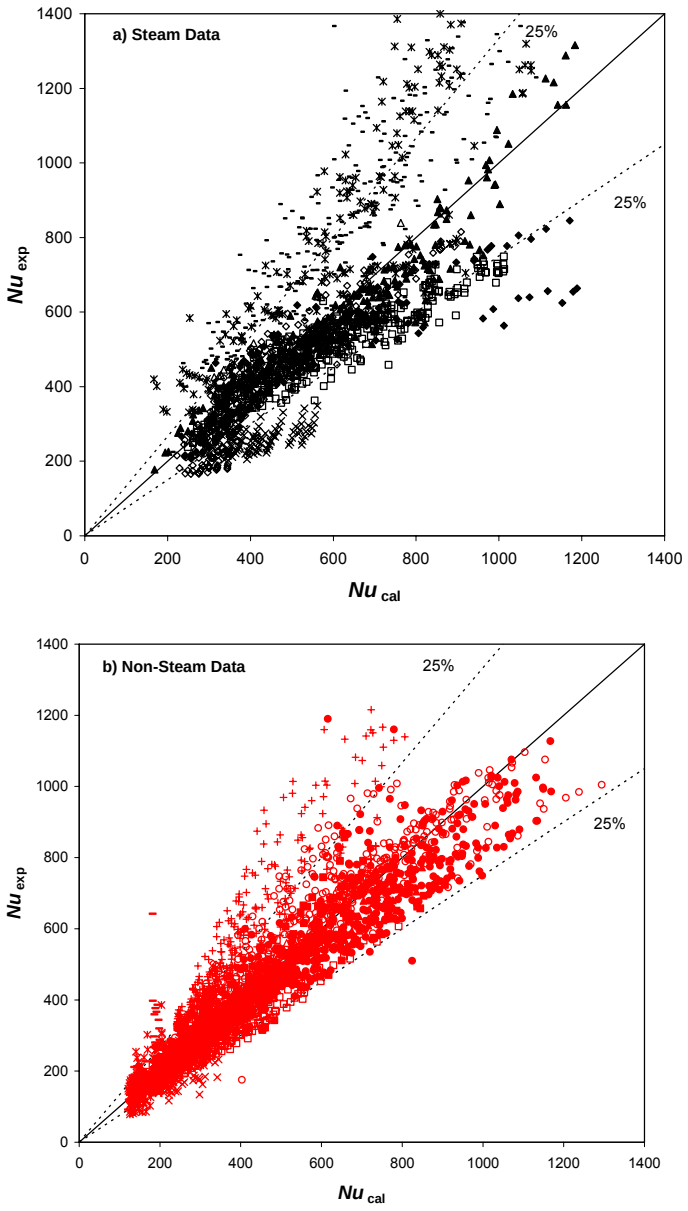

Figure 6 Comparison of Model of Honda et al. [14] to all Data (For key see Table 1)

$$Nu_{\mathrm{sh}} = a_1\left(1 + a_2 A_1\right)^{1/2} A_2 Re_{\mathrm{tp,max}}^{(1-m/2)} Re_{\mathrm{f,u}}^{-n} \qquad (13)$$

where

$$A_1 = Re_{\mathrm{v,max}}^{m}\left(\frac{q}{\rho_v U_{\max} h_{fg}}\right) \qquad (14)$$

$$A_2 = \left(\frac{\rho_{\mathrm{v}}}{\rho}\right)^{1/2}\left(\frac{\nu_{\mathrm{v}}}{\nu}\right)^{m/2} Pr^{0.4} \qquad (15)$$

$$Re_{\mathrm{v,max}} = \rho_{\mathrm{v}} U_{\max} d / \mu_{\mathrm{v}} \qquad (16)$$

The empirical constants a_1, a_2, m and n were found by Honda et al. [14] from their data for R-113 and are given in Table 2. Figure 6b shows good agreement between the Honda et al. [14] model and the non-steam experimental data. The exception again being those of Shah [10] and Kutataladze et al. [11]. For steam data, however, agreement is much less impressive and the data of Briggs and Bui [5] are again particularly poorly predicted.

Table 2 - Values of Empirical Constants in Equations (13 - 16)

Bundles	a_1	a_2	m	n
In-line	0.053	1.83	0.4	0.2
Staggered	$0.165(P_t/P_l)^{0.7}$	18.0	0.2	0.2

Conclusions

Before summing up the performance of the various theoretical models and empirical correlations described above it is worth reappraising the experimental data base in the light of the initial comparisons with theory. In all the comparisons described above the data of Briggs and Bui [5] and Shah [10] have fallen significantly out of line with other data and have been over predicted by all the theories tested. While it is perhaps imprudent to dismiss data simply because it disagrees with theory, in this case the evidence would seem to suggest that these data were effected by air in the test section, due to the low vapour velocities involved. (This was even suggested by Briggs and Bui [5] in their original work.) The data of Kutateladze et al. [11] on the other hand were significantly under predicted by all theories and in addition showed significant scatter, although the reasons for this are less clear. Due to these anomalies, these three data sets will be excluded in what follows. Mean deviations between the remaining experimental data and the various theories and correlations, defined as follows,

$$\text{Mean Deviation} = 100\sqrt{\left\{\frac{1}{N_{tot}}\sum_{1}^{N_{tot}}\left(1 - Nu_{\mathrm{calc}}/Nu_{\mathrm{exp}}\right)\right\}} \qquad (17)$$

are listed in Table 3.

Table 3 - Summary of mean deviations of experimental data (excluding [5], [10] and [11]).

	Shek' and Gom' [16]	Cavallini et al. [19]	McNaught [21]	Honda et al. [14]
Steam	47.6	23.2	26.6	25.2
Non-Steam	28.1	25.6	40.5	15.7
All Data	37.1	24.7	35.6	20.0

Table 4 - Free-Convection Condensation on Integral-Fin Tubes - Experimental Data Base

Reference	Tube Material	Fluid	Number of Geometries	Symbols used In Figures
Wanniarachchi et al. [31]	Copper	Steam	4	■
Yau et al. [32]	Copper	Steam	4	●
Briggs et al. [33]	Copper	Steam	8	△
Briggs et al. [33]	Brass	Steam	8	×
Briggs et al. [33]	Bronze	Steam	8	*
Masuda and Rose [34]	Copper	R113	5	♦
Masuda and Rose [35]	Copper	Ethylene Glycol	4	□
Marto et al. [36]	Copper	R113	19	■
Briggs et al. [33]	Copper	R113	8	▲
Briggs et al. [33]	Brass	R113	8	+
Briggs et al. [33]	Bronze	R113	8	◊

The poor results of the Shekriladze and Gomelauri [16] model are not surprising, since it was developed for single tubes, although the addition of the correction for condensate inundation suggested by Cavallini et al. [19] significantly improves the performance, particularly for the steam data where it is the most successful of the four. The model of Honda et al. [14] is the most successful when compared to the full data base and is particularly effective for non-steam data.

FREE-CONVECTION CONDENSATION ON INTEGRAL-FIN TUBES

When quiescent vapour condenses on an integral-fin tube two mechanisms influence the flow of condensate on, and hence the heat transfer to, the tube. Condensate retention in the inter-fin spaces on the lower part of the tube, as illustrated in Figure 7, leads to a thickening of the condensate film and a decrease in the heat transfer. On parts of the tube not covered by condensate flooding, however, on the fin tips and the flanks and interfin space above the flooding zone, surface tension induced pressure gradients thin the condensate film and enhance the local heat transfer.

Experimental Data Base

Early experimental data (see for example Katz and Geist, [25], Beatty and Katz, [26], Karkhu and Borovkov, [27], Mills et al., [28] and Canarvos, [29]) are difficult to interpret. Details of experimental procedure are often vague and comparison of results is difficult due to the unsystematic choices of geometric variables. Methods of evaluating the vapour-side, heat-transfer coefficient also varied, with some investigators measuring the tube wall temperature and others using indirect methods such as Wilson plots [30]. The accuracy in many cases is difficult to assess. Most of the data, however, showed marked enhancement of heat-transfer coefficients, in most cases greater than the increase in heat-transfer surface area due to the fins.

Due to the uncertainties outlined above, the earlier experimental data will not be used in the current investigation. Table 4 summarise more recent data. While only three fluids are included, namely steam, ethylene glycol and R-113, these give a wide range of thermophysical properties. In addition data are included for over 40 tube geometries and three tube materials.

To quantify the relative performance of finned tubes an enhancement ratio can be defined as follows

$$\varepsilon = \left(\frac{\alpha_{\text{finned}}}{\alpha_{\text{plain}}} \right)_{\text{at same } \Delta T} = \left(\frac{q_{\text{finned}}}{q_{\text{plain}}} \right)_{\text{at same } \Delta T} \qquad (18)$$

Care is needed in the exact definitions of the quantities in equation (18). In the present work, the heat-transfer coefficient (or heat flux) of the finned tube is based on the area of a smooth tube with fin-root diameter while the denominator refers to a plain tube of diameter equal to the fin root diameter of the finned tube. A useful conclusion of the investigations summarized in Table 4 is that for relatively low vapour velocities this enhancement ratio is virtually independent of vapour-side temperature difference.

Other conclusions are:

1) Enhancements ratios are generally higher than increases in surface area, although for condensation of steam this is not always the case.

2) Optimum fin spacings can be identified, and these are dependent on fluid properties.

3) Enhancement ratio increases monotonically with fin height in most cases, although for steam condensing on low thermal conductivity tubes there is little advantage in increasing fin height above about 0.5 mm, due to “fin-efficiency” effects.

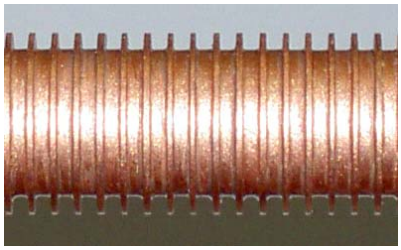

Bare Tube

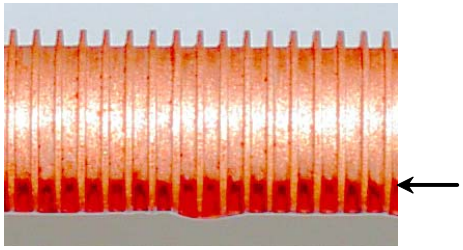

R-113, σ/ρ = 12.4 μNm²/kg

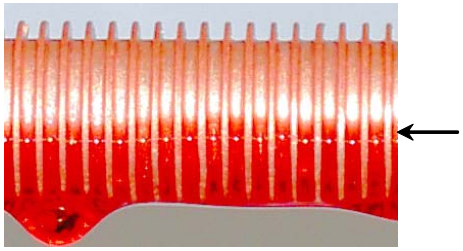

Ethylene Glycol, σ/ρ = 43.5 μNm²/kg

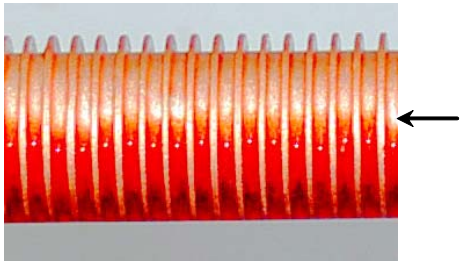

Water, σ/ρ = 72.9 μNm²/kg

Figure 7 Liquid Retention on an Integral-Fin Tube (d = 12.7 mm, t = 0.5 mm, h = 1.6 mm, s = 1.5 mm)

4) Enhancement ratio decreases with fin thickness since thicker fins (with fixed fin spacing) result in reduced fin density.

Gravity Drainage

The enhancements in heat transfer reported, over and above the increase in heat-transfer surface area are not unexpected. In single-phase flows the presence of short surfaces with thin boundary layers produce high local heat-transfer coefficients. The same is true in the case of condensation, where the boundary layer in question is the condensate film, which for a pure saturated vapour, provides the main resistance to heat transfer. The gravity drained models of Nusselt [17] for a vertical surface and a horizontal tube suggest that the heat-transfer coefficient for a vertical fin of height h will surpass that of the bare tube of diameter d by a factor of order.

$$\frac{\alpha_{\text{vertical fin}}}{\alpha_{\text{horizontal tube}}} = \left(\frac{0.943}{0.728}\right)\left(\frac{d}{h}\right)^{1/4} \qquad (19)$$

For low-fin tubes used in condensation this is typically three or more.

Equation (19) formed the basis of the model of Beatty and Katz [26], who simply applied the Nusselt [17] equations for horizontal tubes and vertical plates to the various surfaces on a fined tube. The results are compared to the experimental data base in Figure 8. The model shows good agreement with the non-steam data but less good with the data for steam. This reflect the fact that surface tension, not included in the model, is much higher for water than organic fluids. In particular these data are largely over-predicted by the model, and this is due to the phenomena of condensate flooding.

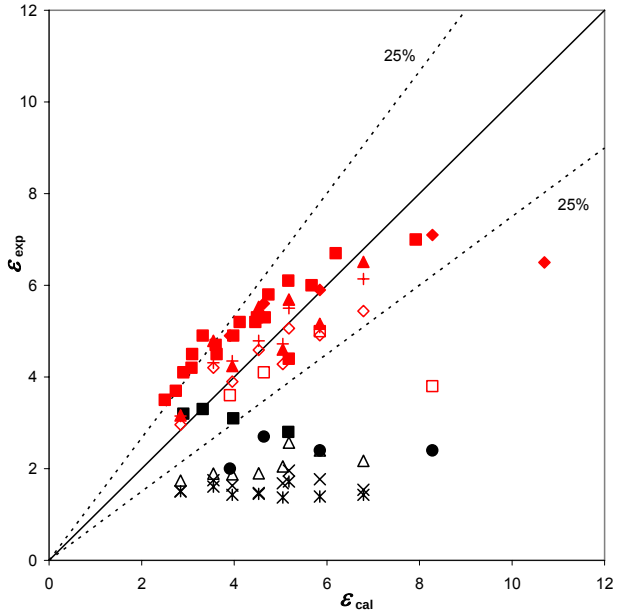

Figure 8 Comparison of Model of Beatty and Katz [26] to Experimental Data (For key see Table 4)

Condensate Flooding

The abrupt thickening of the condensate film between the fins at the so called "flooding" or "retention" angle has been observed by many investigators. The retention angle can be predicted with good accuracy by the following equations, derived independently by Rudy and Webb [37] and Honda et al. [38].

$$\phi_f = \cos^{-1}\left[\frac{4\sigma\cos\beta}{\rho g b d_o} - 1\right] \quad \text{for } b < 2h\cos\beta/(1-\sin\beta) \qquad (20)$$

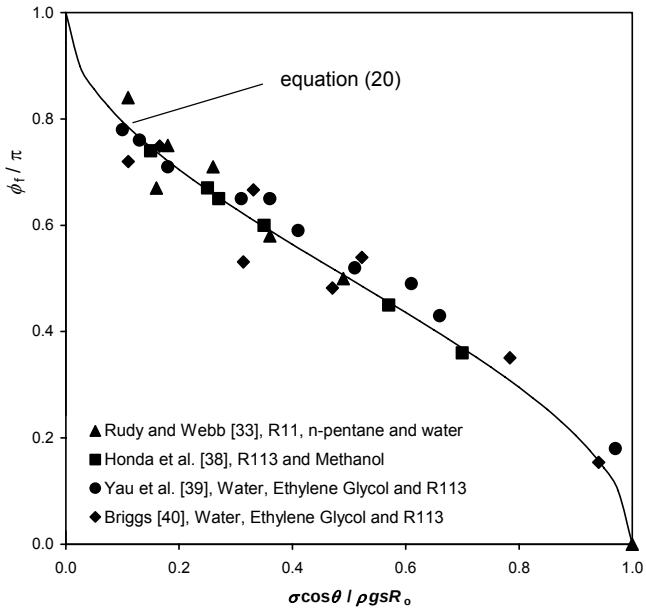

Figure 9 Comparison of Flooding Angle Model to Experimental Data

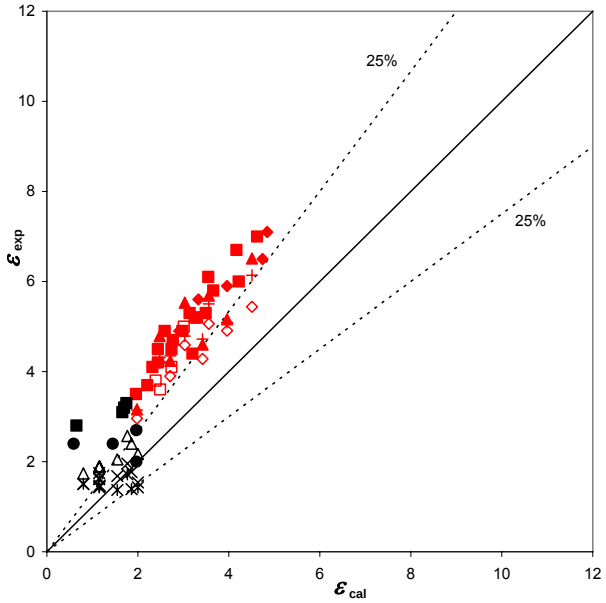

Figure 10 Comparison of Model of Rudy and Webb [37] to Experimental Data (For key see Table 4)

For rectangular cross-section fins this becomes

$$\phi_f = \cos^{-1}\left[\frac{4\sigma}{\rho g b d_o} - 1\right] \qquad \text{for } b < 2h \qquad (21)$$

Figure 9 compares equations (20) with data for a wide range of tube geometries and fluids. It includes measurements for the static case (i.e. without condensation) as well as during condensation.

Rudy and Webb [37] adapted the Beatty and Katz [26] model by simply neglecting heat transfer to the fin flanks and root below the flooding angle (as calculated using equations (20) and (21)). The results are shown in Figure 10, with the majority of the data now above the theoretical prediction. This is because Rudy and Webb [37] neglected the positive effect of surface tension, in that it enhances heat transfer above the flooding zone by thinning the condensate film.

Masuda and Rose [41] showed that liquid is also retained as "wedges" at the fin roots above the retention angle. They developed expressions for rectangular cross-section fins for the proportion of the fin flank and fin root above the flooding angle ϕ_f blanked by these wedges. These expressions were extended by Rose [42] to include trapezoidal cross-section fins as follows

$$f_f = \frac{1-\tan(\beta/2)}{1+\tan(\beta/2)} \cdot \frac{2\sigma\cos\beta}{\rho g d h} \cdot \frac{\tan(\phi_f/2)}{\phi_f} \qquad (22)$$

$$f_s = \frac{1-\tan(\beta/2)}{1+\tan(\beta/2)} \cdot \frac{4\sigma}{\rho g d s} \cdot \frac{\tan(\phi_f/2)}{\phi_f} \qquad (23)$$

Note that for rectangular cross-section fins $\beta = 0$ and the leading term on the right hand sides of equations (22) and (23) are unity.

Surface Tension Enhancement

This phenomena was first pointed out by Gregorig [43]. A non-uniform condensate surface curvature leads to pressure gradients in the film. For one-dimensional curvature the pressure in the liquid exceeds that in the vapour by σ/r, where r is the radius of curvature measured on the liquid side of the interface, so that the pressure gradient along the surface is

$$\frac{dP}{dX} = \sigma \frac{d}{dX}\left(r^{-1}\right) \qquad (24)$$

On a low-fin tube this pressure gradient drives liquid towards the centre of the tip of the fin and along the fin flank and on the interfin tube surface towards the root of the fin, causing the film to thin near the fin tip and on the fin flank and interfin tube space near to the fin root. The consequent reduction in average film thickness enhances heat transfer to the tube.

There have been several attempts to solve this problem for integral-fin tubes based on the Nusselt [17] assumptions and approximations while incorporating the surface tension induced pressure gradient into the momentum equation for the condensate film. Karkhu and Borovkov [27], Rifert [44] and Rudy and Webb [45] assumed linear pressure variation along the fin flank based on assumed radii of curvature at the root and tip of the fin, but these gross approximations yielded little or no improvement over the simple Rudy and Webb [37] model (see Briggs and Rose [46]). The approach of Honda and co-workers [47, 48] is the most complete to date but still contains significant simplifications in order to facilitate numerical solution of the governing, fourth order differential equations for the condensate film thickness. Despite this their approach has given good agreement with experimental data covering a wide range of parameters, as illustrated by Figure 11, which

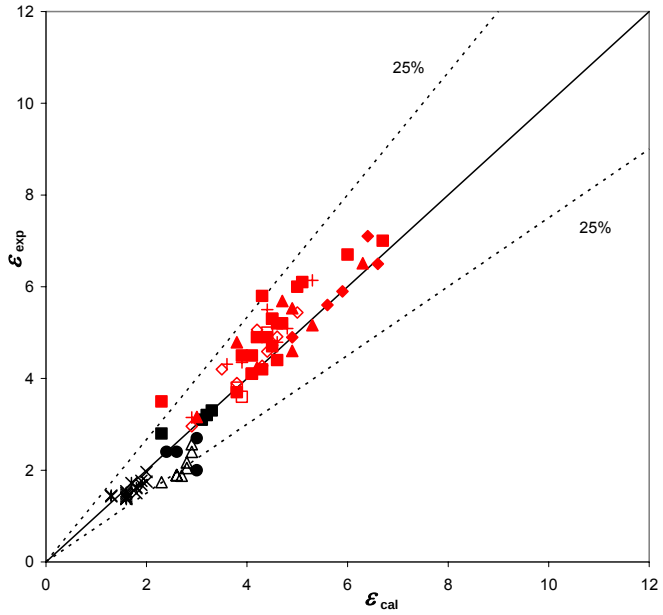

Figure 11 Comparison of Model of Honda et al. [47, 48] to Experimental Data (For key see Table 4)

compares calculated results provided by Honda [49] to the data summarized in Table 4. Note that the model included conduction in the fins and therefore gives good agreement for the low conductivity brass and bronze tubes.

Most recently Wang and Rose [50] formulated the full differential equation for the condensate film thickness over the whole fin and tube surface. While representing an advance on earlier work, however, attempts by the authors to find solutions to these equations were, by their own admission, incomplete.

Semi-Empirical Models

Given the complexities of the problem outlined above, Rose [42] proposed a relatively simple, semi-empirical model for integral-fin tubes for use in design and optimisation. Using a combination of Nusselt [17] for the gravity contribution and dimensional analysis to account for surface tension drainage the following equation was developed for the enhancement ratio of an integral-fin tube.

$$\varepsilon = \left(\left(\frac{d_o}{d} \right)^{3/4} t \left\{ 0.281 + \frac{B\sigma d_o}{t^3 \tilde{\rho} g} \right\}^{1/4} + \frac{\phi_f}{\pi} \left[\frac{1 - f_f}{\cos\beta} \frac{d_o^2 - d^2}{2 h_v^{1/4} d^{3/4}} \left\{ 0.791 + \frac{B\sigma h_v}{h^3 \tilde{\rho} g} \right\}^{1/4} + B_l (1 - f_s) s \left\{ (\xi(\phi_f))^3 + \frac{B\sigma d}{s^3 \tilde{\rho} g} \right\}^{1/4} \right] \right) \Big/ 0.728(b + t) \tag{25}$$

where B and B_l are dimensionless constants, h_v is the "mean vertical fin height", given by

$$h_v = \frac{\phi_f}{\sin(\phi_f)} h \qquad \phi_f \le \frac{\pi}{2} \tag{26}$$

$$h_v = \frac{\phi_f}{1 - \sin(\phi_f)} h \qquad \frac{\pi}{2} < \phi_f \le \pi \tag{27}$$

$\xi(\phi_f)$ results from application of the Nusselt [17] analysis for a horizontal tube above the level of condensate retention, and can be closely approximated by

$$\xi(\phi_f) = 0.874 + 0.1991\text{x}10^{-2}\,\phi_f - 0.2642\text{x}10^{-1}\,\phi_f^2 + 0.5530\text{x}10^{-2}\,\phi_f^3 - 0.1363\text{x}10^{-2}\,\phi_f^4 \tag{28}$$

ϕ_f being calculated from equation (20) or (21), f_f and f_s account for additional condensate retention above the flooding angle and are calculated from equations (22) and (23).

With B = 0.143 and B_l = 2.96, equation (25) gives good agreement with the experimental data base as illustrated in Figure 12. It also gives the correct dependence on fin spacing, thickness and height. The discrepancy between equation (25) and the data for steam condensing on brass and bronze tubes is due to the temperature drop through the fins when the parameter $(\alpha h^2/tk_w)$ becomes large. Briggs and Rose [51] proposed a modification to the model which used "slender fin" theory to account for conduction in the fins. They combined the original semi-empirical equations for heat transfer through the condensate film with one-dimensional conduction through the fins. The resulting algebraic equations were solved iteratively. The results are compared to the experimental data in Figure 13. It can be seen that the correction for temperature drop in the fins successfully pulls the model into line with the data for steam condensing on brass and bronze tubes without significantly affecting the results for the other data which were already in good agreement with the model.

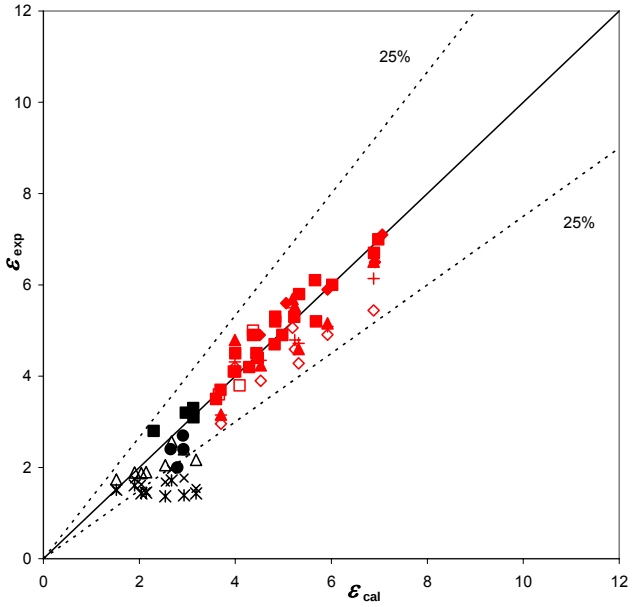

Figure 12 Comparison of Model of Rose [42] to Experimental Data (For key see Table 4)

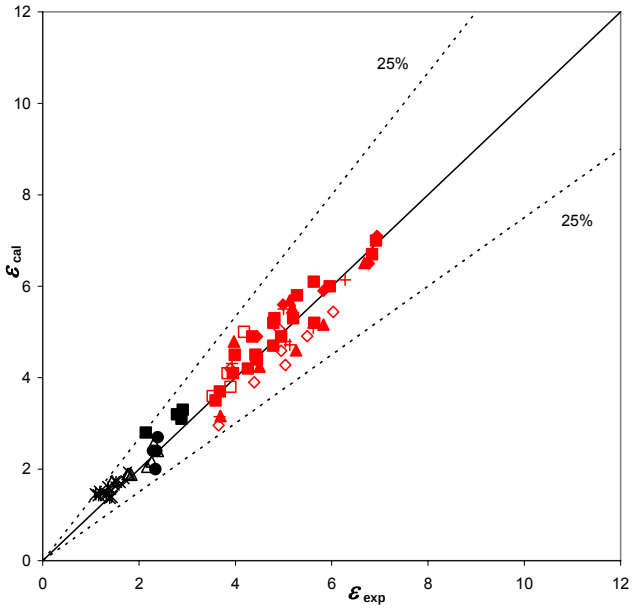

Figure 13 Comparison of Model of Briggs Rose [51] to Experimental Data (For key see Table 4)

FORCED-CONVECTION CONDENSATION ON INTEGRAL-FIN TUBES

The combined effects of gravity, vapour shear and surface tension on condensation on integral-fin tubes has recently received some attention in the literature but as yet the interaction of these effects is far from fully understood.

Experimental Data Base

Table 5 summarises the experimental data available in the open literature. We can extend our definition of enhancement ratio described above to include the additional constraint of equal vapour velocity for finned and plain tube, i.e.

$$\varepsilon = \left(\frac{\alpha_{\text{finned}}}{\alpha_{\text{plain}}}\right)_{\text{same } \Delta T \text{ and } U_v} = \left(\frac{q_{\text{finned}}}{q_{\text{plain}}}\right)_{\text{same } \Delta T \text{ and } U_v} \qquad (29)$$

Early results indicated that for low vapour velocities, the relative increase in heat-transfer coefficient due to vapour velocity was smaller for finned tubes than for plain tubes, resulting in a decrease in enhancement ratio, as defined in equation (30) with increasing vapour velocity.

As more data have become available, however, it is becoming apparent that vapour shear can have an effect on the heat transfer in the flooded section of a finned tube. Bella et al. [58] and Cavallini et al. [59] condensed R-113 and R-11 on three integral-fin tubes with vapour velocities up to 10 m/s. For the two more densely finned tubes (2000 fins per meter) vapour shear affected plain and finned tubes to a similar degree and the enhancement ratio was independent of vapour velocity. Cavallini et al. [59] attributed this to turbulence in the condensate film and "a local reduction of the liquid film thickness in the flooded region".

Namasivayam and Briggs [54-57, 60] tested nine tubes condensing steam at atmospheric and low (14 kPa) pressure and ethylene glycol at low (15 kPa) pressure. For low pressure steam, vapour velocities up to 62 m/s were achieved and the heat-transfer enhancement ratio was found to be a strong function of both vapour velocity and fin spacing. The interrelationship of these two parameters led to complex trends in the data, as illustrated by the sample results in Figure 14. At relatively low velocities the enhancement ratio decreased with increasing vapour velocity in line with results discussed above. At some critical vapour velocity, however, which was different for different fin geometry, vapour shear on the condensate film began to reduce the extent of condensate retention between the fins on the lower part of the tube and this was accompanied in all cases by an increase in the enhancement ratio. Thus the effect of vapour shear on flooding appears to explain, at least qualitatively, the trends observed in Figure 14.

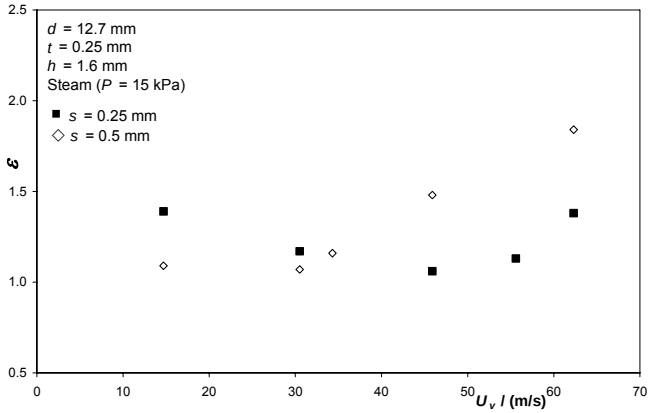

Figure 14 Variation of Enhancement Ratio with Vapour Velocity (Data of Namasivayam and Briggs [56])

Semi-Empirical Models

Cavallini et al. [61] developed a semi-empirical model for forced-convection condensation on integral-fin tubes. The following equation was proposed for the vapour-side, heat-transfer coefficient.

$$\alpha = \left[\alpha_{\text{gr}}^{N} + \alpha_{\text{sh}}^{N}\right]^{\frac{1}{N}} \qquad (30)$$

α_{gr} in equation (30) denotes the vapour-side, heat-transfer coefficient under stationary vapour conditions and was obtained from the model of Briggs and Rose [51]. The second term, α_{sh}, denotes the vapour-side, heat-transfer coefficient when forced-convection dominates and the effects of gravity and surface tension become negligible. This was found from the following correlation.

$$\alpha_{\text{sh}} = C\left(\frac{k}{d_o}\right) Re_{\text{eq}}^{\ 0.8} Pr^{\frac{1}{3}} \qquad (31)$$

where,

$$Re_{\text{eq}} = \left(\frac{\rho_v U_{\max} d_o}{\mu}\right)\left(\frac{\rho}{\rho_v}\right)^{0.5} \qquad (32)$$

Table 5 - Forced-Convection Condensation on Integral-Fin Tubes - Experimental Data Base

Reference	Test Fluid	Pressure / (kPa)	Vapour Velocity / (m/s)	Number of Tubes+	Symbols used in Figures
Michael et al. [52]	Steam	12	4.7 – 31.4	3	◊
Briggs et al. [53]	Steam	3	2.4 – 9.0	3	–
Namasivayam and Briggs [54, 55]	Steam	102	2.3 – 10.4	9	●
Namasivayam and Briggs [56, 57]	Steam	14	14.0 - 62.7	9	△
Michael et al. [52]	R-113	101	0.4 – 1.9	3	+
Briggs et al. [53]	Ethylene Glycol	3	6.9 – 33.3	3	o
Bella et al. [58] Cavallini et al. [59]	R-11	104 - 198	0.2 – 8.7	3*	□
Bella et al. [58] Cavallini et al. [59]	R-113	104 - 198	0.4 – 9.8	3*	■
Namasivayam and Briggs [60]	Ethylene Glycol	15	10.5 – 22.1	9	×

+ All tubes were copper

$$C = 0.03 + 0.166\left(\frac{t}{p}\right) + 0.07\left(\frac{h}{p}\right) \qquad (33)$$

The values of the constants in equation 33, and the value of N (= 2) in Equation 30 were obtained from a best fit procedure using the data of Bella et al. [58] and Cavallini et al. [59] for R-11 and R-113 condensing on 3 tubes. Figure 15 compares results of this model to the experimental data base. The model predicts non-steam data to within 25%. It is less successful, however, at predicting data for steam.

Briggs and Rose [62] also adopted an approach based on equation 30. In this case, however, α_{gr}, was calculated from the model of Rose [42] but with the *observed* flooding angle which in many cases was larger than that calculated using equations (20) or (21), due to vapour shear. (They pointed out that a more complete model would require an equation relating the retention angle to vapour velocity, geometric parameters and condensate properties.)

For α_{sh}, the heat-transfer coefficient for forced convection, it was argued, based on the theoretical results of Wang and Rose [50], that surface tension forces will dominate on the fin flank leaving the fin tip and root as the only areas effected by vapour shear. Furthermore, the fin root will be less affected by vapour shear due to being shielded somewhat by the fins. These arguments led to the following semi-empirical equation for the heat-transfer coefficient for forced convection.

$$\alpha_{sh} = \alpha_{tip}\left(\frac{t}{p}\right)\left(\frac{d_o}{d}\right) + \alpha_{root}\left(\frac{\phi_{obs}}{\pi}\right)\left(\frac{s}{p}\right) \qquad (34)$$

where

$$\alpha_{tip} = \left(\frac{k}{d_o}\right) A \left(\frac{d_o}{d}\right)^a Re_{tp,min}^a \qquad (35)$$

$$\alpha_{root} = \left(\frac{k}{d}\right)\left(1 - \exp\left(-\left(\frac{s}{h}\right)^M\right)\right) A Re_{tp,min}^a \qquad (36)$$

and $Re_{tp,min}$ is the two-phase Reynolds number based on the upstream vapour velocity and the fin root diameter. Equations (35) and (36) are based in part on the model of Shekriladze and Gomelauri [16] for forced-convection condensation, which for a smooth tube gives $Nu = 0.9Re_{tp,min}^{0.5}$. The term $(1\text{-}\exp(\text{-}s/h)^M)$ in equation (36) accounts for the reduced effect of vapour shear at the fin root and, for positive values of M, tends to unity and zero for large and small values of s/h respectively.

The empirical constants, M, n, A and a were found fitting the data summarised in Table 5. This gave the following values; $M = 0.2$, $n = 3$, $A = 2.0$ and $a = 0.5$. The fact that M was found to be positive gives confidence in the form of equation (36).

Figures 16 compares the model to the data base. It can be seen that the present model gives significantly better agreement with the steam data than the model of Cavallini et al. [61]. The non-steam data was well predicted by the model of Cavallini et al [61] since much of it was used in their correlation. The present model is less effective with this data, although agreement is still acceptable.

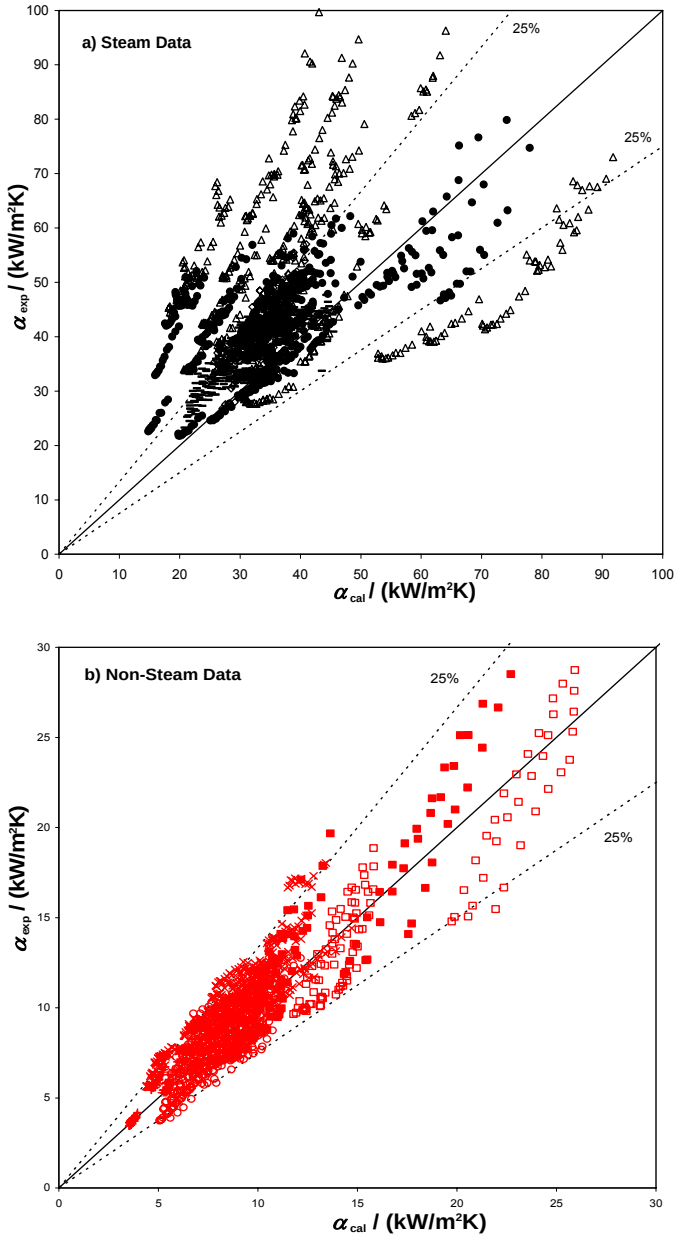

Figure 15 Comparison of Model of Cavallini et al. [61] to Experimental Data (For key see Table 5)

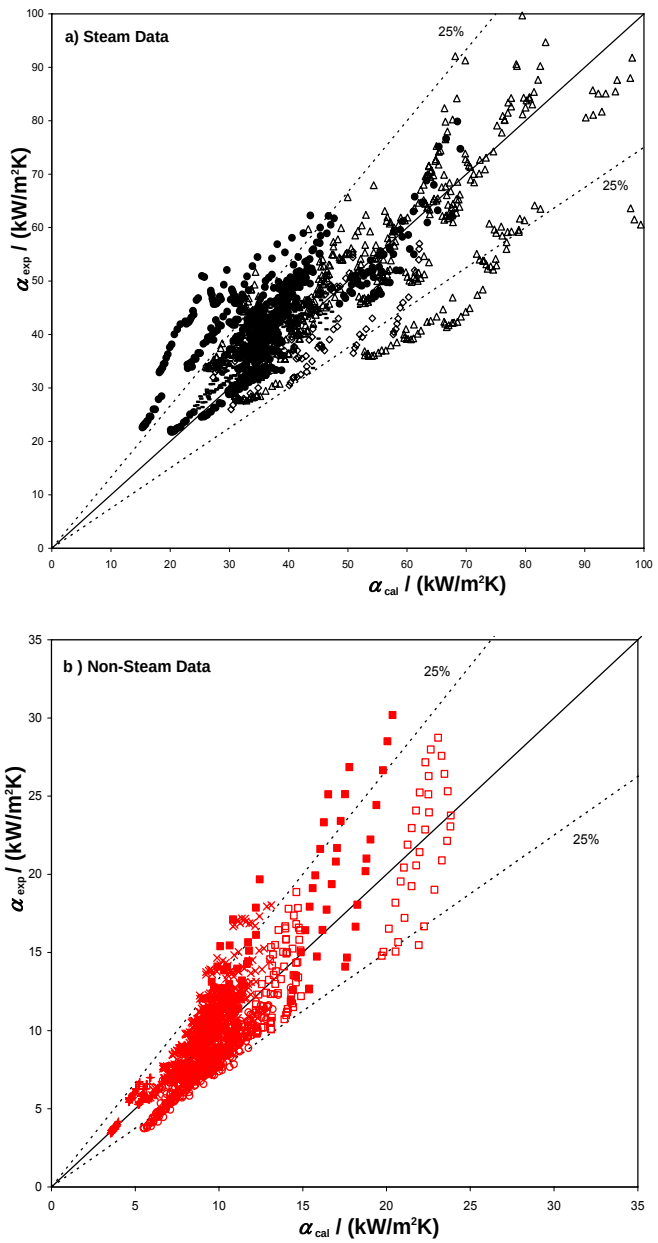

Figure 16 Comparison of Model of Briggs and Rose [62] to Experimental Data (For key see Table 5)

CONCLUSIONS

Condensation on Banks of Plain Tubes

The experimental data base for condensation on banks of plain tubes is summarized in Table 1. The data of [5], [10] and [11] showed poor agreement with the rest of the data and all of the models and correlations evaluated. When these data were excluded, the following conclusions were reached:

For condensation of steam, the models of Cavallini et al. [19], M^{c}Naught [21] and Honda et al. [14] all performed equally well, predicting the data with a mean deviation of about 25%, with the model of Cavallini et al. [19] giving slightly better agreement than the other two. None of the models gave good agreement with the very high velocity data of Michael [2] and Beech [3].

For condensation of vapours other than steam, the correlation of Honda et al. [14] gave easily the best agreement with the data.

None of the models specifically address the issue of turbulence in the condensate film, except in as much as the empirical element of the models include this if it were present in the experimental data used in the correlation. As expected,

this appears to be most prevalent at high vapour shear and high condensate inundation.

Free-Convection Condensation on Integral-Fin Tubes

The mechanisms behind condensation on integral-fin tubes in the absence of significant vapour shear appear to be well understood. These include the effects of condensate retention, surface tension induced enhancement and conduction in the fins. The two most successful models, i.e. those of Honda et al. [47, 48] and Briggs and Rose [51] include all these factors and give very good agreement with the experimental data base summarized in Table 4.

Forced-Convection Condensation on Integral-Fin Tubes

The combined effects of surface tension, gravity and vapour shear on condensation on integral-fin tubes is only recently receiving attention. Experimental data is becoming available and is summarized in Table 5. At present, however, there are no reliable models or correlations available. The effect of vapour shear on the degree of condensate flooding appears to be a major factor in enhancing heat transfer. In addition, the relative effects of surface tension and vapour shear on different areas of the tube surface above the flooding point also needs to be addressed. The correlation of Briggs and Rose [62] attempted to include these factors in a very simple way but with very limited success.

REFERENCES

[1] Nobbs, D. W, The effect of downward vapour velocity and inundation on the condensation rate on horizontal tubes and tube banks, Ph.D. Thesis, University of Bristol, UK, 1975.

[2] Michael, A. G., Lee, W. C. and Rose, J. W., Forced convection condensation of steam on a small bank of horizontal tubes, *Trans ASME J Heat Transfer*, Vol. 114, 1992, pp. 708–713.

[3] Beech, P. M., Filmwise condensation of high velocity downward flowing steam on a bundle of horizontal tubes, Ph.D. These, University of London, UK, 1995.

[4] Briggs, A. and Sabaratnam, S., Condensation of steam in the presence of air on a single tube and a tube bank, *Int. J. Energy Research*, Vol. 27, 2003, pp. 301-314.

[5] Briggs, A. and Bui, H. H., Condensation of steam on banks of tubes - New experimental data and an evaluation of predictive methods, *Proceedings of the 4th Baltic Heat Transfer Conference.,* Kaunas, Lithuania, pp. 499 - 508, 2003.

[6] Gogonin, I. I. and Dorokhov, A. R., Heat transfer from condensing Freon-21 vapour moving over a horizontal tube, *Heat Transfer-Soviet Research*, Vol. 3, 1971, pp. 157-161.

[7] Gogonin, I. I. and Dorokhov, A. R., Experimental investigation of heat transfer with condensation of the moving vapour of Freon-21 on horizontal cylinders, *J. Appl. Mech. Tech. Phys.*, Vol. 17, 1976, pp. 252-257.

[8] Ramamurthy, P. A., Condensation of vapours on a horizontal tube bundle, Ph.D. Thesis, University of Manchester, UK, 1976.

[9] Shah, A. K. Multicomponent condensation on a horizontal tube bank, M.Sc. Thesis, University of Manchester, UK, 1978.

[10] Shah, A. K., Condensation of vapours on a horizontal tube bank, Ph.D. Thesis, University of Manchester, UK, 1981.

[11] Kutateladze, S. S., Gogonin, I. I., Dorokhov, A. R., and Sosunov, V. I., Heat transfer in vapour condensation on a horizontal tube bundle, *Heat Transfer-Soviet Research*, Vol. 13, 1981, pp. 32-50.

[12] Cavallini, A., Frizzerin, S. and Rossetto, L., Refrigerant-11 vapor condensation on a horizontal tube bundle, Rept. No. 121, Inst. di Fisica Tecnica, Universita di Padova, 1985.

[13] Cavallini, A., Frizzerin, S. and Rossetto, L., Refrigerant-113 vapor condensation on a horizontal tube bundle, Rept. No. 133, Inst. di Fisica Tecnica, Universita di Padova, 1988.

[14] Honda, H., Fujii, T., Uchima, B., Nozu, S. and Nakata, S., Condensation of downward flowing R-113 vapour on bundles of horizontal smooth tubes, *Heat Transfer - Japanese Research*, Vol. 18, 1989, pp. 31-52.

[15] Briggs, A., Bui, H. H. and Rose, J. W., Condensation of refrigerant on banks of smooth and finned tubes, *Proceedings of 20th IIR Int. Cong. of Refrigeration,* Sydney, Australia, Vol. 2, Paper No. 518, pp. 2620 – 2626, 2000.

[16] Shekriladze, I. G. and Gomelauri, V. I., Theoretical study of laminar film condensation of flowing vapor, *Int. J. Heat Mass Transfer*, Vol. 9, 1966, pp. 581-591.

[17] Nusselt, W., Die oblerflachenkondensation des wasserdamfes, *Z. Ver. Dt. Ing*., Vol. 60, 1916, pp. 569-575.

[18] Rose, J. W., Effect of pressure gradient in forced-convection film condensation on a horizontal tube, *Int. J. Heat Mass Transfer*, Vol. 27, 1984, pp. 39-47.

[19] Cavallini, A., Frizzerin, S. and Rossetto, L., Condensation of R-11 vapor flowing downward outside a horizontal tube bundle, *Proceedings of 8th Int. Heat Transfer Conferecne,* San Francisco, USA, Vol. 4, 1986, pp. 1707-1712.

[20] Cipollone, E., Cumo, M., Naviglio, A. and Spezia, U., Condensazione su file di tubi orizzontali per "downflow" del vapore a bassa velocita (condensation on lines of horizontal tubes for downflow of vapour at low velocity), *Atti 38o Congr. Naz. ATI, Bari*, Vol. 1, 1983, pp. 57-99.

[21] McNaught, J. M., Two-phase forced-convection heat transfer during condensation on horizontal tube banks, *Proceedings of 7th Int Heat Transfer Conf*erence, Munich, Germany, Vol. 5, 1982, pp. 125 – 131.

[22] ESDU, Convective heat transfer during cross-flow of fluids over plain tube banks, *Data item No. 73031*, Engineering Sciences Data Unit, London, 1973.

[23] Kutateladze, S. S. and Gogonin, I. I., Heat transfer in film condensation in slowly moving vapor, *Int. J. Heat Mass Transfer*, Vol. 22, 1979, pp. 1593-1599.

[24] Kutateladze, S. S., Gogonin, I. I. and Sosunov, V. I., The influence of condensate flow rate on heat transfer in film condensation of stationary vapor on horizontal tube banks, *Int. J. Heat Mass Transfer*, Vol. 28, 1985, pp. 1011-1018.

[25] Katz, D. L. and Geist, J. M., Condensation on six finned tubes in a vertical row, *Trans. ASME*, 1948, pp. 907-914.

[26] Beatty, K.O. and Katz, D.L., Condensation of vapors on outside of finned tubes, *Chem. Eng. Prog*., Vol. 44, 1948, pp. 55-70.

[27] Karkhu, V.A. and Borovkov, V.P., Film condensation of vapour at finely finned horizontal tubes, *Heat Transfer - Soviet Research*, Vol. 3, 1971, pp. 183-191.

[28] Mills, A. F., Hubbard, G. L., James, R. K. and Tan, C., Experimental study of film condensation on horizontal grooved tubes, *Desalination*, Vol. 16, 1975, pp. 121-133.

[29] Canarvos, T. C., An experimental study: condensing R-11 on augmented tubes, , *Proceedings of 19th Nat. Heat Transfer Conference*, Orlando, USA, ASME paper 80-HT-54, 1980.

[30] Wilson, E. E., Basis for rational design of heat-transfer apparatus, *Trans. ASME*, Vol. 37, 1915, pp. 47-56.

[31] Wanniarachchi, A.S., Marto, P.J. and Rose, J.W., Film condensation of steam on horizontal finned tubes: effect of fin spacing, thickness and height, *Multiphase Flow and Heat Transfer*, ASME HTD-47, 1985, pp. 93-99.

[32] Yau, K.K., Cooper, J.R. and Rose, J.W., Effect of fin spacing on

the performance of horizontal integral-fin condenser tubes, *Trans ASME J. Heat Transfer*, Vol. 107, 1985, pp. 377-383.

[33] Briggs, A., Huang, X. S. and Rose, J. W., An experimental investigation of condensation on integral-fin tubes: effect of fin thickness, height and thermal conductivity, *Proceedings of ASME Nat. Heat Transf. Conf*erence, Portland, USA, HTD-Vol. 308, 1995, pp. 21-29.

[34] Masuda, H. and Rose, J.W., An experimental study of condensation of refrigerant-113 on low integral-fin tubes, *Proceedings of the International Symposium on Heat Transfer ,* Beijing, China, Vol. 2, Paper No.32, 1985, and in *Heat Transfer Science and Technology*, Hemisphere, pp. 480-487, 1987.

[35] Masuda, H. and Rose, J.W., Condensation of ethylene glycol on horizontal finned tubes, *Trans ASME J. Heat Transfer*, Vol. 110 1988, pp. 1019-1022.

[36] Marto, P.J., Zebrowski, D., Wanniarachchi, A.S. and Rose, J.W., An experimental study of R-113 film condensation on horizontal finned tubes, *Trans. ASME J. Heat Transfer*, Vol. 112 1990, pp. 758-767.

[37] Rudy, T.M. and Webb, R.L., Condensate retention on horizontal integral-fin tubing, *Advances in Enhanced Heat Transfer*, *Proceedings of 20th Nat. Heat Transfer Conf*erence, ASME HTD-18, 1981, pp. 35-41.

[38] Honda, H., Nozu, S. and Mitsumori, K., Augmentation of condensation on finned tubes by attaching a porous drainage plate, *Proceedings of ASME-JSME Thermal Eng. Joint Conf*erence, Vol. 3, 1983, pp. 289-295.

[39] Yau, K.K., Cooper, J.R. and Rose, J.W., Horizontal plain and finned condenser tubes: effect of fin spacing and drainage strips on heat transfer and condensate retention, *Trans. ASME J. Heat Transfer*, Vol. 108, 1986, pp. 946-950.

[40] Briggs, A., Liquid retention on three-dimensional pin-fin tubes, *Proceedings of 2nd Int. Exergy, Energy and Environment Symp*osium, Kos, Greece, Paper No IEEES2-171, 2005.

[41] Masuda, H. and Rose, J.W., Static configuration of liquid films on horizontal tubes with low radial fins: implications for condensation heat transfer, *Proc. R. Soc. Lond*., Vol. A410, 1987, pp. 125-139.

[42] Rose, J.W., An approximate equation for the vapour-side heat-transfer coefficient for condensation on low-finned tubes, *Int. J. Heat Mass Transfer*, Vol. 37, 1994, pp. 865-875.

[43] Gregorig, R., Hautkondensation an feingewelten oberflachen bei berucksichtigung oberflachenspannunger, *Z. Angew. Math. Phys*., Vol. 5, 1954, pp. 36-49.

[44] Rifert, V.G., A new method for calculating rates of condensation on finned tubes, *Heat Transf. - Sov. Res*, Vol. 12, 1980, pp. 142-147.

[45] Rudy, T.M. and Webb, R.L., Theoretical model for condensation on horizontal integral-fin tubes, *Am. Inst. Chem. Eng. Symp. Ser. 79*, 1983, pp. 11-18,.

[46] Briggs, A. and Rose, J. W., An evaluation of models for condensation heat transfer on low-finned tubes, *J. Enhanced Heat Transfer*, Vol. 6, 1999, pp. 51 - 60.

[47] Honda, H. and Nozu, S., A prediction method for heat transfer during film condensation on horizontal low integral-fin tubes, *Trans. ASME J. Heat Transfer*, Vol. 109, 1987, pp. 218-225.

[48] Honda, H., Nozu, S. and Uchima, B., A generalised prediction method for heat transfer during film condensation on a horizontal low-finned tube, *Proceedings 2nd ASME-JSME Thermal Eng. Joint. Conf*erence, Vol. 4, 1987, pp. 385-392.

[49] Honda, H.: *Private Communication*, 1994.

[50] Wang, H. S. and Rose, J. W., Theoretical investigation of condensation on low-finned tubes, *Proceedings of Heat SET 2007*, Chambery, France, 2007.

[51] Briggs, A. and Rose, J.W., Effect of "fin efficiency" on a model for condensation heat transfer on a horizontal, integral-fin tube, *Int. J. Heat Mass Transfer*, Vol. 37 suppl.1**,** 1994, pp. 457-463.

[52] Michael, A. G., Marto, P. J., Wanniarachchi, A. S. and Rose, J. W., Effect of Vapour Velocity During Condensation on Horizontal Smooth and Finned Tubes, *Proceedings ASME Winter Annual Meeting*, San Francisco, USA, HTD-Vol. 114, 1989, pp. 1-10.

[53] Briggs, A., Wen, X. L. and Rose, J. W., Accurate heat-transfer measurements for condensation on horizontal integral-fin tubes, *Trans. ASME J. Heat Transfer*, Vol. 114, 1992, pp. 719-726

[54] Namasivayam, S. and Briggs, A., Effect of vapor velocity on condensation of atmospheric pressure steam on integral-fin tubes, *Applied Thermal Engineering*, Vol. 24, 2004, pp. 1353-1364.

[55] Namasivayam, S. and Briggs, A., Condensation of atmospheric pressure steam on integral-fin tubes – Effect of fin height and vapour velocity, *Proceedings of 13th Int. Heat Transfer Conf*erence, Sydney, Australia, 2006, Paper No.CSN-16.

[56] Namasivayam, S. and Briggs, A., Effect of vapor velocity on condensation of low-pressure steam on integral-fin tubes, *Trans. ASME J. Heat Transfer*, Vol. 129, 2007, pp. 1486 - 1493.

[57] Namasivayam, S. and Briggs, A., Effect of fin height and vapor velocity on condensation of low-pressure steam on integral-fin tubes, *In Preparation*.

[58] Bella, A., Cavallini, A., Longo, G. A. and Rossetto, L., Pure vapor condensation of refrigerants 11 and 113 on a horizontal integral-fin tube at high vapor velocity, *Enhanced Heat Transfer*, Vol. 1, 1993, pp. 77-86.

[59] Cavallini, A., Doretti, L., Longo, G. A. and Rossetto, L., Experimental investigation of condensate flow patterns on enhanced surfaces, *Proceedings CFC's, The Day After, IIR International Conference*, Padua, Italy, 1994, pp. 627-634.

[60] Namasivayam, S. and Briggs, A., Condensation of ethylene glycol on integral-fin tubes – effect of fin geometry and vapor velocity, *Trans. ASME J. Heat Transfer*, Vol. 127, 2005, pp. 1197-1206.

[61] Cavallini, A., Doretti, L., Longo, G. A. and Rossetto, L., A new model for forced-convection condensation on integral-fin tubes, *Trans. ASME J. Heat Transfer*, Vol. 118, 1996, pp. 689-693.

[62] Briggs, A. and Rose, J. W., Condensation on integral-fin tubes with special reference to effects of vapour velocity, KEYNOTE Paper, *Advances in Heat Transfer, Proceedings of 5th Baltic Heat Transfer Conf*erence, St. Petersburg, Russia, Vol. 1, 2007, pp. 96-116.